

evMLP: An Efficient Event-Driven MLP Architecture for Vision

Zhentan Zheng*

Institute of Artificial Intelligence and Robotics, Xi'an Jiaotong University

Abstract

Deep neural networks have achieved remarkable results in computer vision tasks. In the early days, Convolutional Neural Networks (CNNs) were the mainstream architecture. In recent years, Vision Transformers (ViTs) have become increasingly popular. In addition, exploring applications of multi-layer perceptrons (MLPs) has provided new perspectives for research into vision model architectures. In this paper, we present evMLP accompanied by a simple event-driven local update mechanism. The proposed evMLP can independently process patches on images or feature maps via MLPs. We define changes between consecutive frames as “events”. Under the event-driven local update mechanism, evMLP selectively processes patches where events occur. For sequential image data (e.g., video processing), this approach improves computational performance by avoiding redundant computations. Through ImageNet image classification experiments, evMLP attains accuracy competitive with state-of-the-art models. More significantly, experimental results on multiple video datasets demonstrate that evMLP reduces computational cost via its event-driven local update mechanism while maintaining output consistency with its non-event-driven baseline. The code and trained models are available at <https://github.com/i-evi/evMLP>.

1. Introduction

Convolutional Neural Networks (CNNs) have achieved remarkable success in vision tasks [5, 19, 26]. By scanning convolutional kernels across entire images, they effectively capture local features while reducing parameters through weight sharing. Over more than a decade of development, CNNs have driven transformative progress across computer vision applications. Recently, Vision Transformers (ViTs) [4] have surpassed CNNs in multiple computer vision tasks by leveraging global modeling capabilities from self-attention mechanisms, emerging as a major research

focus. Additionally, novel architectures employing solely multi-layer perceptrons (MLPs) for image processing via fully-connected layers [20, 21] offer fresh perspectives for the research on vision model architectures.

When vision models process image sequences such as videos, consecutive frames often contain redundant information from unchanged regions. In this paper, we define changed areas between consecutive frames as *event* and focus on patches where events occur. We propose a MLP-based network architecture named evMLP and design a simple *event-driven local update mechanism*, illustrated in Figure 1. An *event threshold* is introduced to determine event occurrence on corresponding patches between consecutive frames. When no event occurs in a patch relative to its corresponding patch in the previous frame, our evMLP can reuse computation results from the prior frame’s corresponding patch. This avoids redundant calculations, thus improving network efficiency.

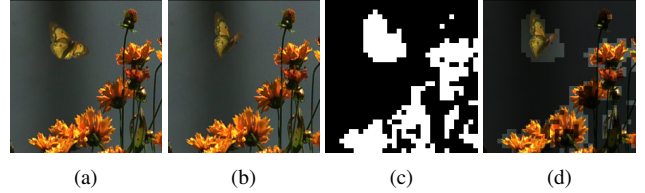


Figure 1. The event-driven local update mechanism. (a) and (b) are two consecutive frames with a resolution of 224×224 . (c) is the event map of (b) relative to (a), with a patch size of 7. White areas indicate regions where events occurred (the calculation of the event map will be explained in Section 3.2). (d) shows (b) masked with the event map. Only the patches in the bright (event) regions need to be recomputed and updated into the precomputed feature map of (a).

The key to implementing our proposed event-driven local update mechanism lies in the model’s ability to process patches on images or feature maps independently. In traditional ViTs or CNNs, processing patches on the image or feature map independently is non-trivial. The attention mechanism is used to model global information in most ViTs, while the convolution kernels of CNNs scan across the entire image or feature map. Therefore, we uti-

*Corresponding author: xjtu_evi@stu.xjtu.edu.cn.

lize MLPs to implement our network architecture. Experimental results demonstrate that our evMLP achieves performance on par with mainstream state-of-the-art network architectures. When trained from scratch on the ImageNet-1K dataset without extra data, it attains 73.6% Top-1 accuracy with a computational cost of 1.3 GMACs per image. Through video processing on multiple datasets, we validated our event-driven local update mechanism. We further conduct experiments to balance computational performance and accuracy via event threshold tuning. Experimental results across multiple video datasets demonstrate that this mechanism enables our evMLP to achieve average computational cost reductions of 7%-14% in general scenarios without compromising accuracy. Notably, in videos captured by stationary cameras, such as surveillance videos, it attains computational cost reductions exceeding 25%. By appropriately increasing the event threshold, the evMLP achieves greater computational efficiency gains while maintaining acceptable accuracy.

2. Related Work

Deep neural networks have demonstrated outstanding performance in computer vision tasks. Since AlexNet [10] achieved revolutionary results in the ImageNet challenge, CNNs have become the mainstream architecture. The convolutional operation can efficiently extract local features of images, such as edges and textures. VGG [16] constructs deep features by stacking 3×3 convolutional kernels, and ResNet [5] breaks through the network degradation problem with residual connections. Through the stacking of deep convolutional layers, the expansion of the parameter scale, and the optimization of the network topology [26] [9] [19], the network architecture with the Convolutional Neural Network (CNN) as the backbone has propelled the achievement of performance breakthroughs in a number of computer vision tasks.

In recent years, ViTs have achieved powerful global context modeling capabilities based on the self-attention mechanism [4, 24]. Employing multi-head attention, ViTs capture both local and global dependencies within images, effectively overcoming the limitations of CNNs' local receptive fields. DeiT [22] addresses ViTs' data-hungry nature via distillation, while Swin Transformer [13] integrates global modeling capabilities with local processing efficiency through a shifted window approach. Architectural innovations in Transformer-based vision models continue to drive performance breakthroughs, surpassing traditional CNNs across diverse computer vision tasks.

Furthermore, recent pure-MLP architectures have achieved competitive performance using exclusively fully-connected layers [20, 21], offering novel perspectives for vision model design. Due to their structural simplicity, MLP-based models frequently attain higher inference through-

put while matching the accuracy of conventional counterparts. Subsequently, numerous MLP-like approaches have demonstrated promising results [1, 7, 12], underscoring MLPs' significant potential as foundational building blocks for vision models.

3. Method

To avoid redundant computation on unchanged information in image sequences, we define changes between consecutive frames as events and propose an event-driven local update mechanism. This mechanism computes only those patches where events have occurred. The key to implementing our proposed event-driven local update mechanism lies in our network's ability to process each patch on an image or feature map independently. Unlike CNNs, where convolutions sweep across the entire image/feature map, or ViTs, which use attention mechanisms to model global relationships, MLPs can straightforwardly process patches on an image or feature map one-by-one. Therefore, we construct our network architecture using MLPs.

3.1. Network Architecture

The overview of the proposed evMLP is illustrated in Figure 2 (a). Given an image or feature map $\mathbf{x} \in \mathbb{R}^{H \times W \times C}$, we divide it into $N \times N$ patches of equal size. Each patch is then flattened into a vector $\mathbf{x}_p \in \mathbb{R}^{C_{in}}$, where $p = 1, 2, \dots, N^2$ and $C_{in} = (H/N) \times (W/N) \times C$. These flattened patches are processed sequentially through the proposed MLP-based building block $\psi(\cdot)$, yielding the transformed outputs $\psi(\mathbf{x}_p) \in \mathbb{R}^{C_{out}}$. By aggregating all processed patches, we obtain a new feature map $\mathbf{x}_{\{\psi(\mathbf{x}_p)\}} \in \mathbb{R}^{N \times N \times C_{out}}$. In this way, each stage of the network independently processes every patch on the feature map, enabling selective computation only for patches where events occur.

Figure 2(b) shows the structure of the proposed building block. The process begins with a fully connected layer that mixes all input information and projects it to the specified dimension C_{out} , followed by n *Inverted Residual Bottlenecks*. Inspired by [8, 15], we employ the inverted residual and bottleneck structure with two fully-connected layers in each Inverted Residual Bottleneck to reduce network parameters: the first layer expands the input d_{in} -dimensional features to $d_{out} = d_{in} \times \alpha$ dimensions through an expansion factor α followed by nonlinear activation, while the second layer projects the features back to d_{in} dimensions and combines them with the input via residual connection before Layer Normalization. In addition, an optional dropout can be added after each nonlinear activation function to prevent the network from overfitting.

3.2. Event-Driven Local Update

We propose an event-driven local update mechanism to improve the computational efficiency of our evMLP for pro-

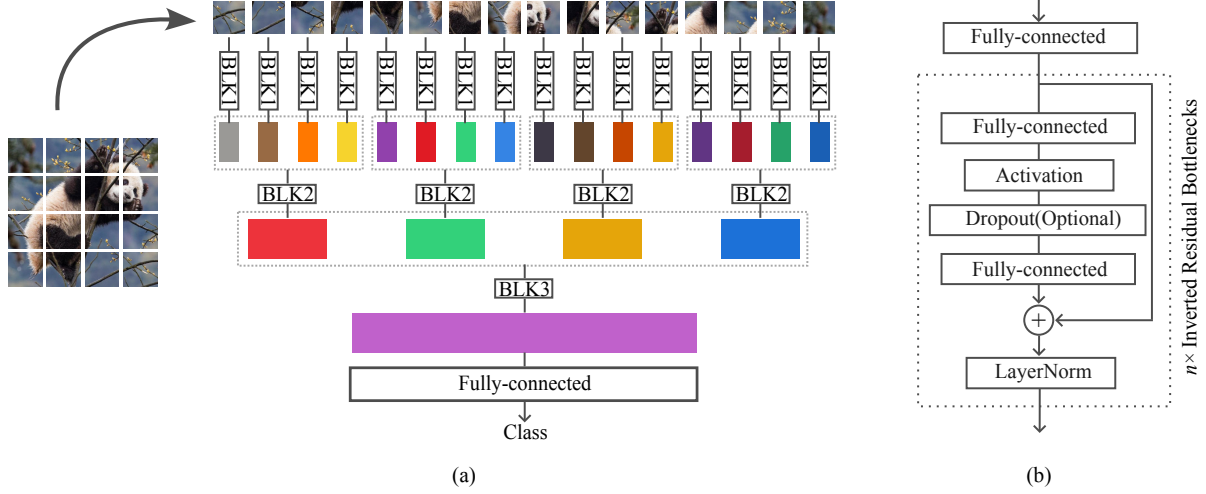


Figure 2. (a) shows the overview of the evMLP’s architecture. The image or feature map is divided into fixed-size patches, and then each patch is processed independently using the proposed MLP-based building blocks. (b) shows the structure of the proposed MLP-based building block, which consists of a fully connected layer followed by n Inverted Residual Bottlenecks. In each Inverted Residual Bottleneck, an activation function is applied after the first fully-connected layer, while the output of the second fully-connected layer undergoes a residual connection with the input data before being processed by a Layer Normalization operation for final output.

cessing image sequences, with the core methodology being the avoidance of redundant computation. By computing only the patches where events occur and updating the results into the precomputed feature map from the previous frame, we thus obtain the computation result for the current processing frame.

Let \mathbf{a}^l denote the current image/feature map to process, and \mathbf{b}^l represent the previously processed image/feature map at stage l (when l is 1, \mathbf{a}^1 and \mathbf{b}^1 denote the raw image). For an n -stage network, the image or feature map at the l -th stage is divided into N^{l^2} patches of size $P^l \times P^l$ through a rearrange operation, resulting in $\{\mathbf{a}_p^l\}_{p=1}^{N^{l^2}}$ and $\{\mathbf{b}_p^l\}_{p=1}^{N^{l^2}}$. The difference image \mathbf{d} of the currently processed image \mathbf{a}^1 relative to the previously processed image \mathbf{b}^1 is obtained via $|\mathbf{a}^1 - \mathbf{b}^1|$. Considering the potential presence of noise from various sources in image sequences, we use an indicator function to assign a value of 1 to elements in \mathbf{d} that are greater than or equal to the *event threshold* τ , and 0 to all other values. This yields \mathbf{c}^0 via the operation $\mathbf{c}^0 = \mathbf{d} \cdot \mathbf{1}_{\mathbf{d} \geq \tau}$. Subsequently, average pooling with a stride of P^l is applied as $\mathbf{c}^l \leftarrow \text{AvgPool2D}(\mathbf{c}^{l-1}, P^l)$ to derive the event map \mathbf{c}^l . Patches corresponding to non-zero pixels \mathbf{c}_p^l in \mathbf{c}^l indicate regions where events have occurred. Therefore, the l -th stage $\psi^l(\cdot)$ of the network only needs to process the patches where events occur and update \mathbf{a}_p^{l+1} with $\psi^l(\mathbf{a}_p^l)$. For patches where no event occurs, the corresponding feature \mathbf{a}_p^{l+1} does not need to be calculated; instead, the result \mathbf{b}_p^{l+1} from the previous frame can be directly reused. By avoiding redundant calculations in this way, the computational efficiency can be improved. The so proposed event-

driven local update mechanism is summarized in Algorithm 1.

Algorithm 1 Event-driven local update mechanism

```

1:  $\mathbf{d} \leftarrow |\mathbf{a}^1 - \mathbf{b}^1|$ 
2:  $\mathbf{c}^0 = \mathbf{d} \cdot \mathbf{1}_{\mathbf{d} \geq \tau}$ 
3: for  $l = 1$  to  $n$  do
4:    $\{\mathbf{a}_p^l\}_{p=1}^{N^{l^2}} \leftarrow \mathbf{a}^l, \{\mathbf{b}_p^l\}_{p=1}^{N^{l^2}} \leftarrow \mathbf{b}^l$ 
5:    $\mathbf{c}^l \leftarrow \text{AvgPool2D}(\mathbf{c}^{l-1}, P^l)$ 
6:   for  $p = 1$  to  $N^{l^2}$  do
7:     if  $\mathbf{c}_p^l \neq 0$  then
8:        $\mathbf{a}_p^{l+1} \leftarrow \psi^l(\mathbf{a}_p^l)$ 
9:     else
10:       $\mathbf{a}_p^{l+1} \leftarrow \mathbf{b}_p^{l+1}$ 
11:    end if
12:  end for
13:   $\mathbf{a}^{l+1} \leftarrow \{\mathbf{a}_p^{l+1}\}_{p=1}^{N^{l^2}}$ 
14: end for

```

4. Experiments

We evaluate the performance of the proposed evMLP on image classification tasks, and demonstrate the efficacy of our event-driven local update mechanism through computational cost analysis in video processing. Controlled experiments further examine how event threshold settings trade off accuracy against computational efficiency.

4.1. Implement Details

Following the architecture in Section 3.1, we implement evMLP for image classification. The network takes $224 \times 224 \times 3$ inputs, processes them through 6 stages of our evMLP’s building block to generate $1 \times 1 \times 512$ feature maps, and produces k -dimensional outputs via a fully-connected layer. We employ GELU [6] activation functions, with dropout applied to randomly zero features at tuned probabilities for mitigating overfitting. Configurations are detailed in Table 1.

Table 1. Specifications for evMLP. BLK denotes our evMLP’s building block described in Section 3.1. FC denotes fully-connected. P denotes the patch size, α denotes the expansion factor, d_{out} denotes the output dimension, and n denotes the number of residual blocks in the BLK.

Input	Operator	P	α	C_{out}	n	Dropout
$224^2 \times 3$	BLK	7	4	64	5	0
$32^2 \times 64$	BLK	2	4	128	5	0
$16^2 \times 128$	BLK	2	4	512	5	0
$8^2 \times 512$	BLK	2	4	512	5	0
$4^2 \times 512$	BLK	2	4	512	5	0
$2^2 \times 512$	BLK	2	4	512	5	0.2
$1^2 \times 512$	FC	-	-	k	-	-

4.2. ImageNet Classification

We evaluated our evMLP on the ImageNet-1K [3] dataset, which contains a training set of 1.28 million images across 1000 categories and a validation set of 50,000 images. We train our model from scratch using PyTorch [14] with the SGD optimizer with momentum. We use a momentum of 0.9, weight decay of $1e^{-5}$, batch size of 1024, and initial learning rate of 0.1. We employed a cosine scheduler to decay the learning rate over 300 epochs, incorporating a linear warm-up for the first 5 epochs. Augmentation and regularization strategies similar to those in [4, 20, 23] were adopted, including auto-augment, label smoothing, mixup, cutmix, and random erasing.

We compare the classification performance of our evMLP with several mainstream state-of-the-art architectures on the ImageNet-1K validation set. Since our evMLP model has relatively low computational cost, we compared it with models [5, 22, 27] which have similar computational cost (measured by MACs). For reference, we also include higher-computational-cost models [4, 20]. All models are trained from scratch without extra data with 224×224 input resolution. The comparison results are shown in Table 2. Experimental results demonstrate that our evMLP model achieves the highest Top-1 accuracy of 73.6% at a computational cost of 1.3 GMACs, under comparable levels of com-

Table 2. Performance comparisons of various models on the ImageNet-1K validation set, all models are trained from scratch without extra data. Models above the middle rule require lower computational cost, while those below incur higher computational cost. Throughput is measured on an NVIDIA TITAN RTX GPU, using the GitHub repository provided in [25].

Model	MACs (G)	Params (M)	Throughput (imgs/sec)	Top-1 Acc
ResNet18 [5]	1.8	11.6	3371	69.7%
T2T-ViT-7 [27]	1.1	4.3	1637	71.7%
DeiT-Ti [22]	1.0	5.6	2671	72.2%
evMLP	1.3	46.8	2693	73.6%
ViT-16B [4]	11.2	58.1	291	79.6%
Mixer-B/16 [20]	12.6	59.9	379	76.4%

putational cost. Additionally, it remains competitive with models exceeding 10 GMACs in computational cost.

4.3. Computational Cost Analysis for Video Processing

Our proposed evMLP utilize an event-driven local update mechanism to process only the patches where events occur within the image sequence, thereby improving computational efficiency. Video processing serves as an effective way to validate our event-driven local update mechanism. We process videos in the video datasets HMDB51 [11], MSVD [2], UCF101 [17], and UCF-Crime [18] using our evMLP (for UCF-Crime, only the testing set is utilized), comparing the computational performance of the model with and without the event-driven local update mechanism. We set the event threshold τ (refer to Section 3.2) to 0, meaning any pixel change is considered an event occurrence. This ensures that using the event-driven local update mechanism does not affect the processing results, allowing us to focus solely on changes in computational cost. Frames in the videos are resized to 224×224 and processed frame-by-frame. We report and compare the average MACs per frame processed by our evMLP model with and without the event-driven local update mechanism across multiple datasets, as shown in Table 3.

Experimental results show that our proposed event-driven local update mechanism improves the computational performance of our evMLP across diverse video datasets. For Action Recognition datasets HMDB51 and UCF101 (relatively simple scenes), computational cost decreased by 13.6% and 13.5%, reducing the average per-frame cost from 1.287 GMACs to 1.111 GMACs and 1.113 GMACs. For Video Description dataset MSVD (richer scenes), the improvement was more modest with a 7.7% computational cost reduction, yielding an average of 1.2 GMACs per

Table 3. Comparison of computational cost (MACs(G)/frame) with/without the event-driven local update mechanism across video datasets. \times denotes the baseline without the event-driven local update mechanism, while \checkmark represents the case with the mechanism enabled, where the event threshold $\tau = 0$.

	evMLP \times	evMLP \checkmark
HMDB51 [11]	1.287	1.111(\downarrow 13.6%)
MSVD [2]	1.287	1.187(\downarrow 7.7%)
UCF101 [17]	1.287	1.113(\downarrow 13.5%)
UCF-Crime [18]	1.287	0.964 (\downarrow 25.1%)

frame. On surveillance dataset UCF-Crime (stationary cameras, reduced camera-motion *events*), computational performance significantly improves, with a 25.1% reduction in average per-frame computational cost, achieving an average of 0.964 GMACs per frame.

4.4. Study of the Event Threshold

Consecutive video frames often exhibit noise that is semantically irrelevant to image content. Under stringent event thresholds, however, corresponding patches may be erroneously flagged as containing events and consequently updated. Moreover, by virtue of deep neural networks’ robust generalization capabilities, semantically insignificant variations may exert negligible influence on computational outcomes. While experiments in Section 4.3 validate the efficacy of the event-driven local update mechanism, conservatively configuring the event threshold at $\tau = 0$ – albeit ensuring output consistency with the non-event-driven baseline – fails to yield substantial computational efficiency improvements. In this section we study the impact of event threshold configurations on evMLP’s computational efficiency and accuracy.

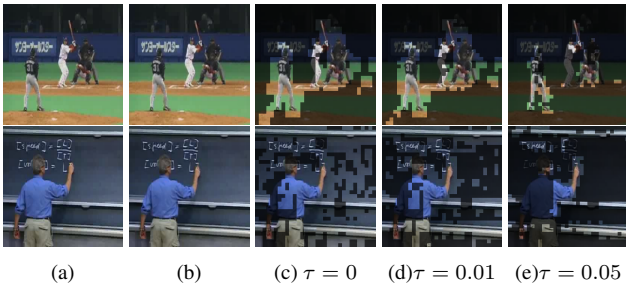
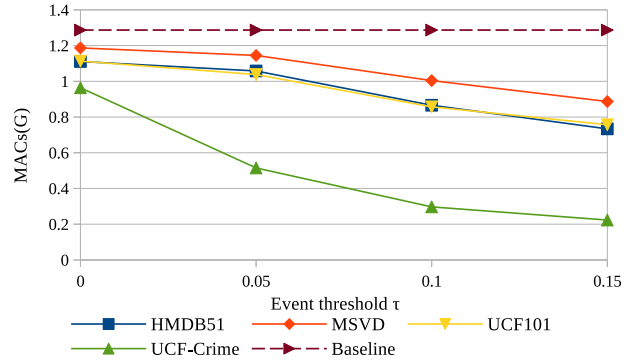


Figure 3. Comparison of event maps generated with different event thresholds. (a), (b) are consecutive video frames. (c)-(e) are results of event maps generated using different event thresholds τ and superimposed on frame (b), brighter areas indicate patches where events occur.

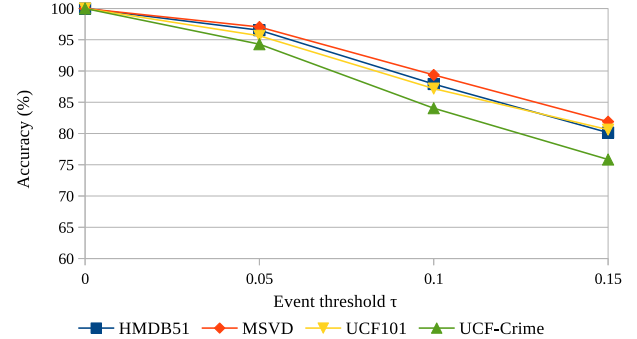
Figure 3 visualizes event maps generated under differ-

ent event thresholds, demonstrating that aggressive threshold settings significantly reduce event regions – thereby improving computational performance – whereas excessively large thresholds may neglect authentic events, potentially compromising processing outcomes. When the event threshold τ is set to 0, evMLP yields identical results to its operation without the event-driven local update mechanism. Therefore, we establish the frame-by-frame processing results at $\tau = 0$ as the ground truth. This enables quantitative evaluation of event threshold impact by comparing accuracy rates of different thresholds against the $\tau = 0$ baseline.

We apply the ImageNet-1K [3] pre-trained evMLP model with varying event thresholds to multiple video datasets including HMDB51 [11], MSVD [2], UCF101 [17], and UCF-Crime [18] (for UCF-Crime, only the testing set is utilized). During experimentation, video frames are resized to 224×224 and fed into the model to produce classification outputs. As shown in Fig. 4, varying event thresholds ($\tau \in \{0, 0.05, 0.1, 0.15\}$) significantly impact both per-frame computational cost (GMACs/frame) and accuracy across all evaluated datasets.



(a) Impact of event thresholds on computational cost across datasets, the non-event-driven baseline is plotted as a dashed line for comparison.



(b) Impact of event thresholds on model accuracy across datasets.

Figure 4. Impact of event thresholds on accuracy and computational cost across datasets, $\tau \in \{0, 0.05, 0.1, 0.15\}$.

Experimental results demonstrate that increasing the

event threshold classifies more patches as event-inactive. Under our event-driven local update mechanism, computation for these patches is skipped, thus reducing computational cost while correspondingly decreasing accuracy. At $\tau = 0.05$, computational cost reductions exceeding 10% are achieved across all datasets while maintaining accuracy above 90%. When τ increases to 0.15, aggressive event thresholds yield significant computational savings surpassing 30% on all datasets, yet reduce accuracy to unacceptably low levels near 80%. Additionally, as plotted, our evMLP featuring the event-driven local update mechanism shows significant performance differences across datasets - Section 4.5 discusses these variations.

4.5. Cross-Dataset Performance Variations

Results in Section 4.4 exhibit substantial performance variations across datasets, discussed herein. As HMDB51 [11] and UCF101 [17] are action recognition datasets, results on these datasets show similar computational performance and accuracy trends under varying event thresholds. Results on dataset UCF-Crime [18] demonstrate significant computational improvements but more pronounced accuracy degradation. Conversely, results on dataset [2] exhibit limited computational gains with relatively contained accuracy reduction. We therefore focus our analysis on the UCF-Crime and MSVD scenarios.

The stationary camera recordings avoid camera-motion artifacts, enabling our evMLP to achieve significantly superior computational performance on UCF-Crime at identical event thresholds compared to other datasets. At $\tau = 0.05$, the average per-frame computational cost reduces to 0.515 GMACs/frame - less than half the baseline (1.287 GMACs/frame) while maintaining an accuracy of 94.285%. With increasing τ , the improvement in computational performance on dataset UCF-Crime remains significantly ahead of that on other datasets. However, excessive update skipping—while improving computational efficiency—substantially compromises accuracy. At $\tau = 0.15$, computational cost on UCF-Crime reduces by over 80% to an average of 0.223 GMACs/frame, whereas accuracy drops to 75.843%, while maintaining above 80% on other datasets. Results on dataset MSVD exhibit more conservative performance gains. As a video description dataset featuring diverse scenes and moving cameras, frequent inter-frame events are generated. At $\tau = 0.05$, our evMLP achieves merely 11% computational improvement on it. Although the model delivers superior outcomes on MSVD versus other datasets at identical thresholds, at $\tau = 0.15$ it reduces computational cost to 0.887 GMACs/frame while diminishing accuracy to 81.89%.

5. Conclusion

In this paper, we present all-MLP architecture evMLP featuring a simple event-driven local update mechanism. We implement evMLP and evaluate its performance on ImageNet classification, demonstrating accuracy comparable to state-of-the-art models. Video processing experiments demonstrate that through our proposed event-driven local update mechanism, our evMLP is capable of reducing computational cost without compromising performance by avoiding redundant computations. Furthermore, by adjusting the event thresholds, evMLP can balance the model’s computational efficiency and accuracy using the event-driven local update mechanism. Experiments across multiple video datasets have shown that in stationary camera scenarios, our event-driven local update mechanism achieves the best performance improvements.

References

- [1] Guiping Cao, Shengda Luo, Wenjian Huang, Xiangyuan Lan, Dongmei Jiang, Yaowei Wang, and Jianguo Zhang. Strip-mlp: Efficient token interaction for vision MLP. In *IEEE/CVF International Conference on Computer Vision, ICCV 2023, Paris, France, October 1-6, 2023*, pages 1494–1504. IEEE, 2023. 2
- [2] David L. Chen and William B. Dolan. Collecting highly parallel data for paraphrase evaluation. In Dekang Lin, Yuji Matsumoto, and Rada Mihalcea, editors, *The 49th Annual Meeting of the Association for Computational Linguistics: Human Language Technologies, Proceedings of the Conference, 19-24 June, 2011, Portland, Oregon, USA*, pages 190–200. The Association for Computer Linguistics, 2011. 4, 5, 6
- [3] Jia Deng, Wei Dong, Richard Socher, Li-Jia Li, Kai Li, and Li Fei-Fei. Imagenet: A large-scale hierarchical image database. In *2009 IEEE Computer Society Conference on Computer Vision and Pattern Recognition (CVPR 2009)*, 20-25 June 2009, Miami, Florida, USA, pages 248–255. IEEE Computer Society, 2009. 4, 5
- [4] Alexey Dosovitskiy, Lucas Beyer, Alexander Kolesnikov, Dirk Weissenborn, Xiaohua Zhai, Thomas Unterthiner, Mostafa Dehghani, Matthias Minderer, Georg Heigold, Sylvain Gelly, Jakob Uszkoreit, and Neil Houlsby. An image is worth 16x16 words: Transformers for image recognition at scale. In *9th International Conference on Learning Representations, ICLR 2021, Virtual Event, Austria, May 3-7, 2021*. OpenReview.net, 2021. 1, 2, 4
- [5] Kaiming He, Xiangyu Zhang, Shaoqing Ren, and Jian Sun. Deep residual learning for image recognition. In *2016 IEEE Conference on Computer Vision and Pattern Recognition, CVPR 2016, Las Vegas, NV, USA, June 27-30, 2016*, pages 770–778. IEEE Computer Society, 2016. 1, 2, 4
- [6] Dan Hendrycks and Kevin Gimpel. Gaussian error linear units (gelus). *CoRR*, abs/1606.08415, 2016. 4
- [7] Qibin Hou, Zihang Jiang, Li Yuan, Ming-Ming Cheng, Shuicheng Yan, and Jiashi Feng. Vision permutator: A per-

- mutable mlp-like architecture for visual recognition. *IEEE Trans. Pattern Anal. Mach. Intell.*, 45(1):1328–1334, 2023. [2](#)
- [8] Andrew Howard, Ruoming Pang, Hartwig Adam, Quoc V. Le, Mark Sandler, Bo Chen, Weijun Wang, Liang-Chieh Chen, Mingxing Tan, Grace Chu, Vijay Vasudevan, and Yukun Zhu. Searching for mobilenetv3. In *2019 IEEE/CVF International Conference on Computer Vision, ICCV 2019, Seoul, Korea (South), October 27 - November 2, 2019*, pages 1314–1324. IEEE, 2019. [2](#)
- [9] Gao Huang, Zhuang Liu, Laurens van der Maaten, and Kilian Q. Weinberger. Densely connected convolutional networks. In *2017 IEEE Conference on Computer Vision and Pattern Recognition, CVPR 2017, Honolulu, HI, USA, July 21-26, 2017*, pages 2261–2269. IEEE Computer Society, 2017. [2](#)
- [10] Alex Krizhevsky, Ilya Sutskever, and Geoffrey E. Hinton. Imagenet classification with deep convolutional neural networks. In Peter L. Bartlett, Fernando C. N. Pereira, Christopher J. C. Burges, Léon Bottou, and Kilian Q. Weinberger, editors, *Advances in Neural Information Processing Systems 25: 26th Annual Conference on Neural Information Processing Systems 2012. Proceedings of a meeting held December 3-6, 2012, Lake Tahoe, Nevada, United States*, pages 1106–1114, 2012. [2](#)
- [11] Hildegard Kuehne, Hueihan Jhuang, Estíbaliz Garrote, Tomaso A. Poggio, and Thomas Serre. HMDB: A large video database for human motion recognition. In Dimitris N. Metaxas, Long Quan, Alberto Sanfeliu, and Luc Van Gool, editors, *IEEE International Conference on Computer Vision, ICCV 2011, Barcelona, Spain, November 6-13, 2011*, pages 2556–2563. IEEE Computer Society, 2011. [4, 5, 6](#)
- [12] Hanxiao Liu, Zihang Dai, David R. So, and Quoc V. Le. Pay attention to mlps. In Marc’Aurelio Ranzato, Alina Beygelzimer, Yann N. Dauphin, Percy Liang, and Jennifer Wortman Vaughan, editors, *Advances in Neural Information Processing Systems 34: Annual Conference on Neural Information Processing Systems 2021, NeurIPS 2021, December 6-14, 2021, virtual*, pages 9204–9215, 2021. [2](#)
- [13] Ze Liu, Yutong Lin, Yue Cao, Han Hu, Yixuan Wei, Zheng Zhang, Stephen Lin, and Baining Guo. Swin transformer: Hierarchical vision transformer using shifted windows. In *2021 IEEE/CVF International Conference on Computer Vision, ICCV 2021, Montreal, QC, Canada, October 10-17, 2021*, pages 9992–10002. IEEE, 2021. [2](#)
- [14] Adam Paszke, Sam Gross, Francisco Massa, Adam Lerer, James Bradbury, Gregory Chanan, Trevor Killeen, Zeming Lin, Natalia Gimelshein, Luca Antiga, Alban Desmaison, Andreas Köpf, Edward Z. Yang, Zachary DeVito, Martin Raison, Alykhan Tejani, Sasank Chilamkurthy, Benoit Steiner, Lu Fang, Junjie Bai, and Soumith Chintala. Pytorch: An imperative style, high-performance deep learning library. In Hanna M. Wallach, Hugo Larochelle, Alina Beygelzimer, Florence d’Alché-Buc, Emily B. Fox, and Roman Garnett, editors, *Advances in Neural Information Processing Systems 32: Annual Conference on Neural Information Processing Systems 2019, NeurIPS 2019, December 8-14, 2019, Vancouver, BC, Canada*, pages 8024–8035, 2019. [4](#)
- [15] Mark Sandler, Andrew G. Howard, Menglong Zhu, Andrey Zhmoginov, and Liang-Chieh Chen. Mobilenetv2: Inverted residuals and linear bottlenecks. In *2018 IEEE Conference on Computer Vision and Pattern Recognition, CVPR 2018, Salt Lake City, UT, USA, June 18-22, 2018*, pages 4510–4520. Computer Vision Foundation / IEEE Computer Society, 2018. [2](#)
- [16] Karen Simonyan and Andrew Zisserman. Very deep convolutional networks for large-scale image recognition. In Yoshua Bengio and Yann LeCun, editors, *3rd International Conference on Learning Representations, ICLR 2015, San Diego, CA, USA, May 7-9, 2015, Conference Track Proceedings*, 2015. [2](#)
- [17] Khurram Soomro, Amir Roshan Zamir, and Mubarak Shah. UCF101: A dataset of 101 human actions classes from videos in the wild. *CoRR*, abs/1212.0402, 2012. [4, 5, 6](#)
- [18] Waqas Sultani, Chen Chen, and Mubarak Shah. Real-world anomaly detection in surveillance videos. In *2018 IEEE Conference on Computer Vision and Pattern Recognition, CVPR 2018, Salt Lake City, UT, USA, June 18-22, 2018*, pages 6479–6488. Computer Vision Foundation / IEEE Computer Society, 2018. [4, 5, 6](#)
- [19] Mingxing Tan and Quoc V. Le. Efficientnet: Rethinking model scaling for convolutional neural networks. In Kamalika Chaudhuri and Ruslan Salakhutdinov, editors, *Proceedings of the 36th International Conference on Machine Learning, ICML 2019, 9-15 June 2019, Long Beach, California, USA*, volume 97 of *Proceedings of Machine Learning Research*, pages 6105–6114. PMLR, 2019. [1, 2](#)
- [20] Ilya O. Tolstikhin, Neil Houlsby, Alexander Kolesnikov, Lucas Beyer, Xiaohua Zhai, Thomas Unterthiner, Jessica Yung, Andreas Steiner, Daniel Keysers, Jakob Uszkoreit, Mario Lucic, and Alexey Dosovitskiy. Mlp-mixer: An all-mlp architecture for vision. In Marc’Aurelio Ranzato, Alina Beygelzimer, Yann N. Dauphin, Percy Liang, and Jennifer Wortman Vaughan, editors, *Advances in Neural Information Processing Systems 34: Annual Conference on Neural Information Processing Systems 2021, NeurIPS 2021, December 6-14, 2021, virtual*, pages 24261–24272, 2021. [1, 2, 4](#)
- [21] Hugo Touvron, Piotr Bojanowski, Mathilde Caron, Matthieu Cord, Alaaeldin El-Nouby, Edouard Grave, Gautier Izacard, Armand Joulin, Gabriel Synnaeve, Jakob Verbeek, and Hervé Jégou. Resmlp: Feedforward networks for image classification with data-efficient training. *IEEE Trans. Pattern Anal. Mach. Intell.*, 45(4):5314–5321, 2023. [1, 2](#)
- [22] Hugo Touvron, Matthieu Cord, Matthijs Douze, Francisco Massa, Alexandre Sablayrolles, and Hervé Jégou. Training data-efficient image transformers & distillation through attention. In Marina Meila and Tong Zhang, editors, *Proceedings of the 38th International Conference on Machine Learning, ICML 2021, 18-24 July 2021, Virtual Event*, volume 139 of *Proceedings of Machine Learning Research*, pages 10347–10357. PMLR, 2021. [2, 4](#)
- [23] Hugo Touvron, Matthieu Cord, Matthijs Douze, Francisco Massa, Alexandre Sablayrolles, and Hervé Jégou. Training data-efficient image transformers & distillation through attention. In Marina Meila and Tong Zhang, editors, *Proceed-*

ings of the 38th International Conference on Machine Learning, ICML 2021, 18-24 July 2021, Virtual Event, volume 139 of *Proceedings of Machine Learning Research*, pages 10347–10357. PMLR, 2021. 4

- [24] Ashish Vaswani, Noam Shazeer, Niki Parmar, Jakob Uszkoreit, Llion Jones, Aidan N. Gomez, Lukasz Kaiser, and Illia Polosukhin. Attention is all you need. In Isabelle Guyon, Ulrike von Luxburg, Samy Bengio, Hanna M. Wallach, Rob Fergus, S. V. N. Vishwanathan, and Roman Garnett, editors, *Advances in Neural Information Processing Systems 30: Annual Conference on Neural Information Processing Systems 2017, December 4-9, 2017, Long Beach, CA, USA*, pages 5998–6008, 2017. 2
- [25] Ross Wightman. Pytorch image models. <https://github.com/rwightman/pytorch-image-models>, 2019. 4
- [26] Saining Xie, Ross B. Girshick, Piotr Dollár, Zhuowen Tu, and Kaiming He. Aggregated residual transformations for deep neural networks. In *2017 IEEE Conference on Computer Vision and Pattern Recognition, CVPR 2017, Honolulu, HI, USA, July 21-26, 2017*, pages 5987–5995. IEEE Computer Society, 2017. 1, 2
- [27] Li Yuan, Yunpeng Chen, Tao Wang, Weihao Yu, Yujun Shi, Zihang Jiang, Francis E. H. Tay, Jiashi Feng, and Shuicheng Yan. Tokens-to-token vit: Training vision transformers from scratch on imagenet. In *2021 IEEE/CVF International Conference on Computer Vision, ICCV 2021, Montreal, QC, Canada, October 10-17, 2021*, pages 538–547. IEEE, 2021. 4